CONF-960994-2

SAN096-0879C
SAND--96-0879C

Interaction of cavities with misfit dislocations in SiGe/Si heterostructures

D. M. Follstaedt, S. M. Myers, J. A. Floro and S. R. Lee

Sandia National Laboratories

Albuquerque, NM 87185-1056

Abstract

Consequences of the strong, short-range attractive interaction between cavities and misfit dislocations are examined in SiGe/Si heterostructures. When He is implanted at the SiGe/Si interface, either in situ during epitaxial growth or by post-growth treatment, cavities form and locate on the misfit dislocation cores. The misfit dislocations are no longer straight lines extending over several microns, but form a network with jogs and intersections at the cavities. The He-implanted cavity layer enhances thermal relaxation of the strained alloy and may increase the achievable degree of relaxation by lowering dislocation energies.

1. Introduction

Ion-implantation of He into semiconductors has been shown to form bubbles that can be degassed during subsequent annealing, leaving behind empty cavities [1,2]. The cavities are being evaluated for uses in microelectronic devices, such as gettering metallic impurities [2-5] or altering electronic properties of semiconductors [6]. Several observations with transmission electron microscopy (TEM) indicate an attractive interaction between cavities and dislocations in the damaged layer formed by the He implantation [7]. Moreover, calculations using elastic continuum theory indicate that the binding between cavities and dislocations is quite strong, e.g. ~600 eV for a 10-nm radius cavity centered on a screw dislocation core in Si, and is of short

DISCLAIMER

range [8]. We supposed that cavities might significantly alter the relaxation of strained epitaxial overlayers through this interaction. Our initial investigation showed that placing the He-induced cavity layer at the interface of a strained SiGe/Si heterostructure significantly enhanced its thermal relaxation rate [7].

Here we examine the effects of a cavity layer on the microstructures of misfit dislocations in SiGe/Si heterostructures. The He was introduced either in situ during molecular beam epitaxy (MBE) growth or into pre-grown, fully strained heterostructures by subsequent implantation. Cavities formed at the interface intersect misfit dislocations and disrupt their propagation in straight lines that would extend several micrometers in relaxed, unimplanted alloys. Three structures with increasing degrees of cavity/misfit-dislocation interaction are discussed below. Cross-section specimens for TEM were prepared by conventional metallographic polishing and ion milling techniques; plan-view specimens were similarly prepared by back-thinning. The composition and strain relaxation of the alloy overlayers were determined by x-ray diffraction.

2. In Situ He Implantation during MBE

Specimens were implanted in situ by adding a low-energy He ion gun to a MBE chamber. Growth was done at 550°C, but halted to implant $2x10^{16}$ He/cm^2 at 4.5 kV followed by annealing 1/2 hour at 700°C to outgas and enlarge the resulting cavities. Shown in Fig. 1 is a specimen for which a Si buffer layer was grown on (001) Si, cavities were formed, and then the $Si_{83}Si_{17}$ alloy was grown to a thickness of ~300 nm. This placed most cavities below the SiGe overlayer as seen in cross-section in Fig. 1a. Examination at higher magnification shows a distribution of cavities: smaller cavities (≈4 nm in diameter) are found ~20 nm below the interface and larger

cavities (≈12 nm) are found beneath them, extending to ~65 nm below the interface. A few cavities and some dislocations resulting from implantation damage touch the interface.

The cavity layer has minimal effect on the microstructure of the misfit dislocations, as seen in the plan-view, weak-beam image in Fig. 1b. The specimen is thinnest at the bottom of Fig. 1b but includes the interface. The cores of individual misfit dislocations are in contrast and seen to extend in straight lines over several micrometers. The vertical set of misfit dislocations in Fig. 1b have stronger contrast than the second, orthogonal set, as expected for 60° dislocations. The specimen is thicker in the middle and upper parts of Fig. 1b, and additional dislocations from the deeper He-implanted region appear as meandering curves superimposed on the straight misfit dislocations. Other plan-view images show most cavities located on these implantation-damage dislocations, as expected from the cross-section images. This specimen illustrates the short-range nature of the interaction: cavities ≳20 nm below the interface do not greatly perturb misfit dislocations. The alloy's in-plane lattice constant was relaxed 61% from its fully strained value toward the value of the Si substrate, consistent with the high density of misfit dislocations. Based on examinations of similar specimens without He treatment and cross-section images of this specimen, we expect that the misfit dislocations were nucleated by growth-related inhomogeneities in the epilayers and possibly by the implanted layer.

In the specimen seen in Fig. 2, the $Si_{83}Ge_{17}$ alloy was grown to 50 nm thickness, the cavity treatment was applied, and then growth of the SiGe layer was continued to a thickness of 275 nm. By pre-growing a SiGe layer nearly equal to the He implantation depth and then implanting, a layer of larger cavities up to 20 nm in diameter forms at the interface, as seen in cross-section in Fig. 2a; smaller cavities are also found up to 45 nm in above of it. This specimen was found

to be 66% relaxed, comparable to the specimen discussed above. However, the corresponding weak-beam image in Fig. 2b no longer shows extended, straight misfit dislocations; some sections appear nearly straight but only over distances $\lesssim 1$ μm. Dislocations appearing as irregular curves or extended loops are also seen and probably result from the implantation damage. This second specimen shows that when cavities are positioned at the interface, they disrupt the extension of misfit dislocations. The shorter length is likely due to both an increased nucleation density of misfit dislocations and glide retardation at cavity-dislocation intersections.

3. Implantation of an Existing Heterostructure

We also implanted He at the interface of an existing fully strained $Si_{86}Ge_{14}$ alloy grown on (001) Si by chemical vapor deposition [9]. A dose comparable to that above, 1.7×10^{16} He/cm^2, was implanted at 30° incidence from normal at 15 keV. Annealing 1 hour at 900°C produced 54% relaxation of the heterostructure. The cross-section image in Fig. 3a shows an $\approx$50 nm-thick layer of cavities centered on the interface, with dislocations along the layer and some threading through the overlayer to the surface. This anneal temperature is higher than that used with in situ growth, and the cavities are correspondingly larger, 10-30 nm in diameter.

The increased thermal evolution at 900°C allowed the cavities to interact with misfit and other dislocations to a greater degree, and this is indicated by the plan-view, weak-beam image in Fig. 3b. Extended, straight misfit dislocations are no longer seen; instead the microstructure is a network of short dislocation segments whose cores (imaged with weak-beam conditions) intersect cavities and often change direction. Individual segments between cavities are ~100 nm long; occasionally some segments align into a straight sections which are $\lesssim$300 nm long. This

specimen demonstrates that when cavities are placed at the interface and given sufficient thermal mobility to interact, they greatly disrupt the misfit dislocation microstructure.

4. Discussion

The cavity-dislocation interaction energy was estimated [8] by first evaluating the strain energy that would have been in the cavity volume and multiplying the result by a factor of 1.5-2.0 to account for matrix strain relaxation about the open volume. The dislocation core energy was included by the usual approach of adjusting the inner cutoff radius of the strain integral [10]. The factor of 1.5-2.0 was deduced from elastic continuum calculations for exactly solvable geometries. Such calculations also indicate that dislocation strain fields are significantly altered only in regions immediately around a cavity. This short-range alteration is supported by dark-field images of cavities and dislocations with the weak-beam condition relaxed somewhat to illuminate part of the strain fields around dislocations. An example from the pre-grown heterostructure is seen in Fig. 3c. Many cavities simply remove the illuminated strain contrast and appear as sharply defined dark holes. In other cases where the dislocation strain field is only weakly illuminated, the edge of the cavity is highlighted in white. Both contrasts indicate that the strain fields are modified only locally near the edge of a cavity. It appears clear that significant modification is limited to less than about one radius beyond the cavity.

Cavities appear able to influence heterostructure relaxation in two ways. First, thermal relaxation proceeds more rapidly, presumably due to increased nucleation sites for misfit dislocations. Control specimens of the $Si_{86}Ge_{14}$ heterostructure without implantation were annealed 1 hour at 900°C as above but showed negligible change; to achieve relaxation (19-61%) similar to the implanted specimens, 1 hour at 1000°C was used [7]. Cross-section images such

as Fig. 4 from the unimplanted specimen show dislocations at the interface, extending into the substrate, and threading through the overlayer. Notably, a narrow cavity layer placed at the interface produces relaxation without dislocations protruding into the substrate [7]. Second, the degree of relaxation may be increased when cavities are bound to misfit dislocations. Detailed measurements indicate that dislocations in the pregrown heterostructure have ~1/5 of their core length passing through cavities. If the energy of the misfit dislocations is then reduced by 1/5, the relaxation at equilibrium balance between strain energy and dislocation energy [10] is calculated to increase from 76% to 80%. Anneals of the He-implanted heterostructure at 1000°C produce relaxations of 79-81% that agree with this value.

This work was supported by the United States Department of Energy under contract DE-AC04-94Al85000.

5. References

1. C. C. Griffioen, J. H. Evans, P. C. de Jong and A. Van Veen, Nucl. Inst. Meth. **B27** (1987) 417.

2. D. M. Follstaedt, S. M. Myers, G. A. Petersen and J. W. Medernach, J. Elect. Mat. **25** (1996) 151.

3. S. M. Myers, D. M. Follstaedt, H. J. Stein, C. H. Seager and W. R. Wampler, Nucl. Inst. Meth. **B106** (1995) 379.

4. J. Wong-Leung, E. Nygren and J. S. Williams, Appl. Phys. Lett. **67** (1995) 416.

5. V. Rainieri, P. G. Fallica, G. Percolla, A. Battaglia, M. Barbagallo and S. U. Campisano, J. Appl. Phys. **78** (1995) 1.

6. C. H. Seager, S. M. Myers, R. A. Anderson, W. L. Warren and D. M. Follstaedt, Phys. Rev. **B50** (1994) 2458.

7. D. M. Follstaedt, S. M. Myers and S. R. Lee, Applied Physics Letters, in press.

8. S. M. Myers, unpublished work.

9. Specimen was grown by ultrahigh vacuum/chemical vapor deposition as in B. S. Myerson, Appl. Phys. Lett. **48** (1986) 797.

10. J. Y. Tsao, *Materials Fundamentals for Molecular Beam Epitaxy* (Academic Press, Boston, 1993).

Figure Captions

Figure 1. TEM images of $Si_{83}Ge_{17}$ grown on Si by MBE after in situ He implantation. a) Bright-field image in cross-section, and b) Dark-field, weak-beam g = (220) image in plan-view.

Figure 2. TEM images of $Si_{83}Ge_{17}$ grown on Si by MBE; growth was interrupted after 50 nm for in situ He implantation and then continued. a) Bright-field image in cross-section, and b) Dark-field, weak-beam g = (220) image in plan-view.

Figure 3. TEM images of $Si_{86}Ge_{14}$ heterostructure that was implanted with He and annealed 1 hour at 900°C. a) Bright-field image in cross-section, b) Dark-field, weak-beam g = (220) image in plan-view, and c) Dark-field, plan-view image with increased diffraction.

Figure 4. Bright-field, cross-section image of the $Si_{86}Ge_{14}$ heterostructure with no implantation after 1 hour at 1000°C.

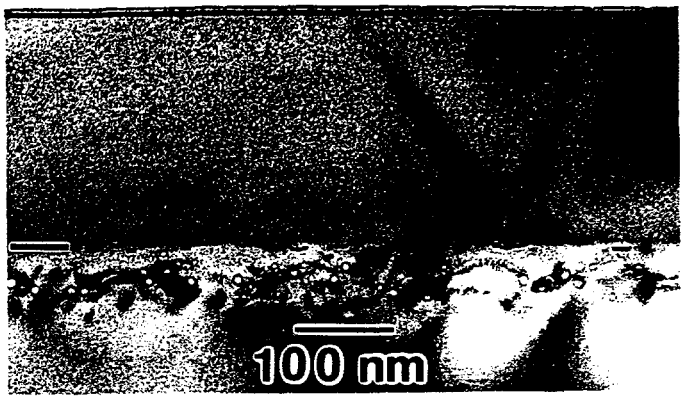

1a

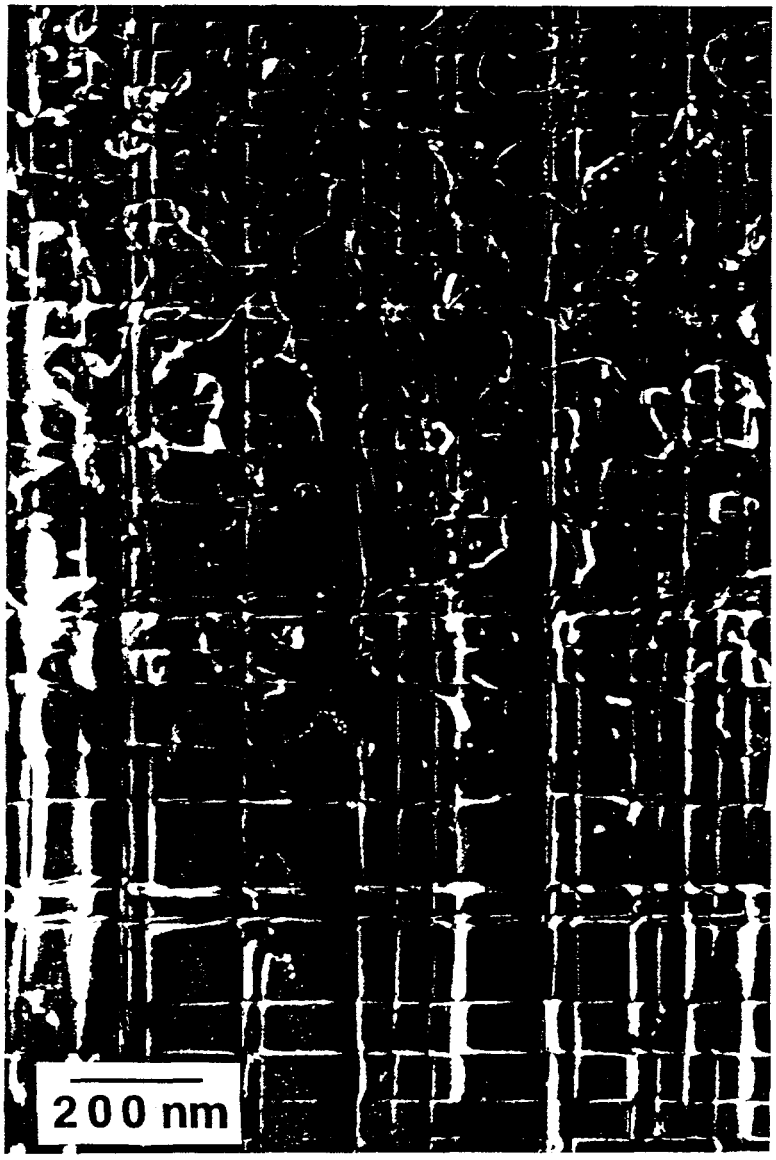

1b

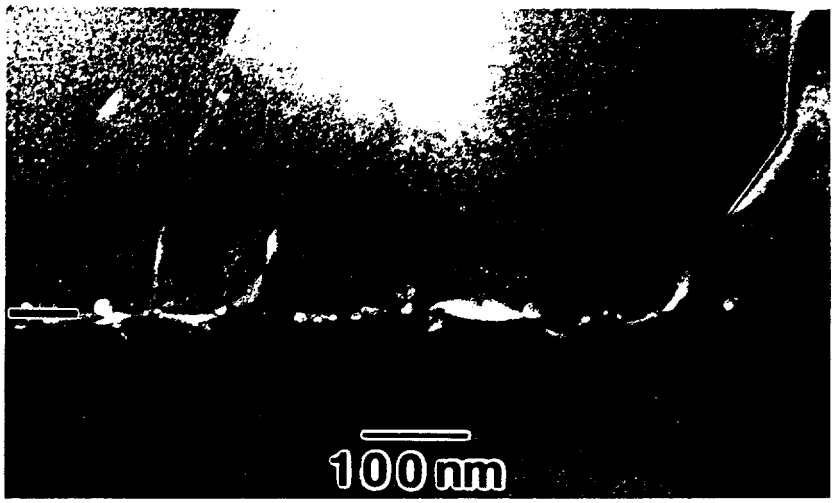

2a

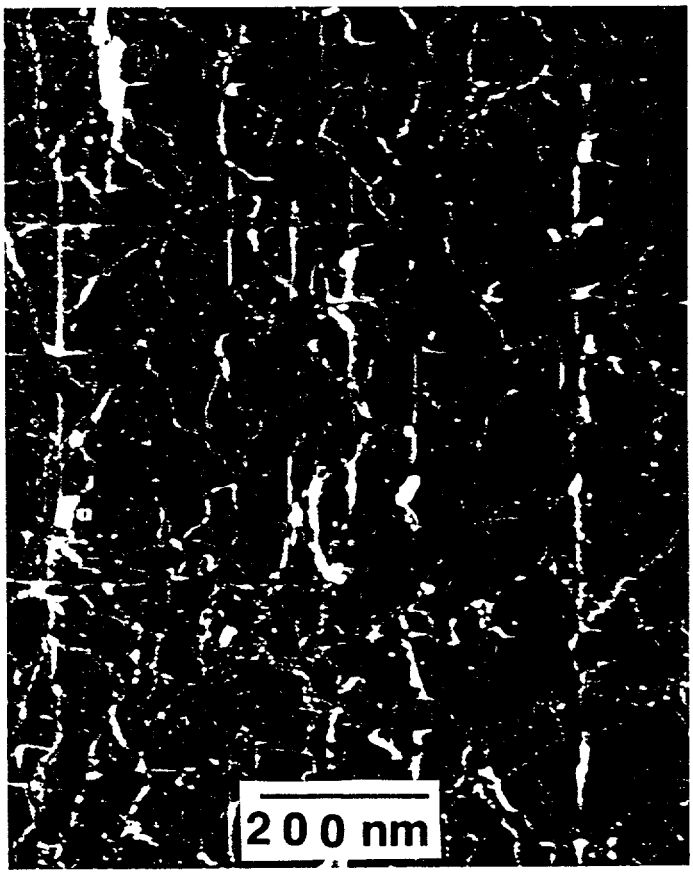

2b

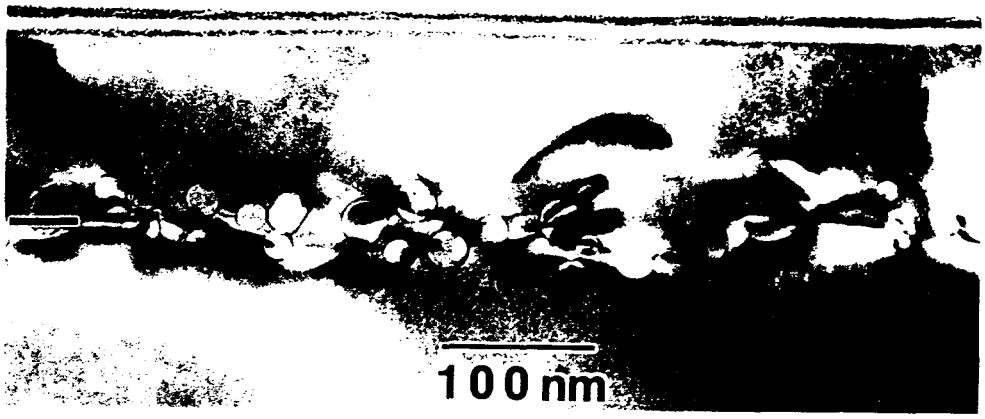

3a

3b

3C

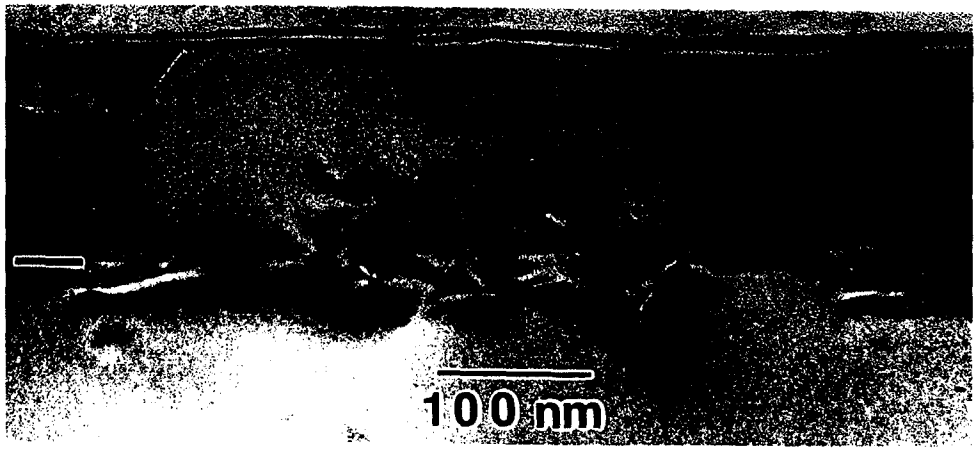

4